Topics in Catalysis Vol. 46, Nos. 1–2, September 2007 (© 2007)
DOI: 10.1007/s11244-007-0332-6

Molecular adsorption on $V_2O_3(0001)/Au(111)$ surfaces

Athula Bandara[a], Mohammad Abu-Haija[a], Frank Höbel[a], Helmut Kuhlenbeck[a], Günther Rupprechter[a,b,*], and Hans-Joachim Freund[a]

[a]*Department of Chemical Physics, Fritz Haber Institute, Faradayweg 4–6, 14195 Berlin, Germany*
[b]*Institute of Materials Chemistry, Vienna University of Technology, Veterinärplatz 1, 1210 Vienna, Austria*

The adsorption of carbon monoxide (CO), propane (C_3H_8) and propene (C_3H_6) on $V_2O_3(0001)$ films grown on Au(111) was studied by Temperature Programmed Desorption (TPD) and X-ray Photoelectron Spectroscopy (XPS). The "oxidized" surface (i.e., as prepared exhibiting V = O termination), the "reduced" surface (i.e., V = O groups being removed by electron irradiation), as well as the oxygen pre-covered reduced surface were investigated. Both TPD and XPS indicate that the oxidized surface has little affinity for CO adsorption, while the reduced surface readily binds CO (CO amount approx. 10 times higher). Accordingly, CO can be used to titrate the presence or absence of vanadyl oxygen (via adsorption on the vanadium atoms) but also of defects like surface oxygen vacancies. For propane and propene, desorption of the parent molecules was the major process, i.e., surface reactions were absent under the applied conditions. When oxygen was pre-adsorbed on the reduced surface, the adsorption properties resembled that of the oxidized surface, i.e., the vanadyl groups were (partially) re-established. TPD and XPS provide a handle to differentiate the binding sites on the V_2O_3 surface.

KEY WORDS: vanadium oxide; carbon monoxide; propane; propene; temperature-programmed desorption; photoelectron spectroscopy; catalysis.

1. Introduction

Vanadium oxides are widely used in heterogeneous catalysis, e.g., for (oxidative) dehydrogenation of alkanes, oxidation of methanol, manufacture of important chemicals, etc [1–8]. The oxidation state of vanadium and the variability in the oxygen coordination play a central role in the catalytic performance of vanadium oxides [1–10]. V_2O_5 supported on other oxides such as Al_2O_3, SiO_2, TiO_2, ZrO_2 and CeO_2 is the most used vanadium system for catalytic reactions [1,4–7,11,12]. However, the role of vanadium oxides in catalytic reactions remains a controversial issue since their exact surface structure and composition is an open question (particularly under reaction conditions), which is in part due to difficulties in the characterization of high surface area catalyst materials. Thin films of vanadium oxides, grown in ultrahigh vacuum on suitable substrates, are an alternative route to study the properties of oxide surfaces. A number of groups have reported procedures to prepare well-defined vanadium oxide thin films of varying stoichiometry. For instance, V_2O_3 has been prepared on various substrates (Pd(111), Au(111) and W(110)) and was characterized by Low Energy Electron Diffraction (LEED), X-ray Photoelectron Spectroscopy (XPS), Scanning Tunneling Microscopy (STM), Near Edge X-ray Absorption Fine Structure (NEXAFS), High Resolution Electron Energy Loss Spectroscopy (HREELS) and other methods (e.g. [13–24]). Netzer and co-workers reported variations in surface termination, availability of oxygen vacancies and stability of V_2O_3 surfaces [13–18]. Vanadium oxide thin films were also used to study the adsorption of small molecules [13–24] and a number of Density Functional Theory (DFT) studies were reported [25–29]. Vanadium oxide islands on noble metals are also known to enhance the rate of CO hydrogenation. Hayek and coworkers studied this phenomenon on "inverse model catalysts" (such as VO_x overlayers on Rh(111) and Rh foil [30]) as well as on Rh nanoparticles supported by thin films of V_2O_3 [31].

Studies on $V_2O_3(0001)$ films in our laboratory [19,32,33], combining STM, HREELS, IRAS and XPS have shown the formation of a V-terminated surface upon electron irradiation. The vibrational data revealed that the V = O vibration vanished after electron radiation and STM indicated that the surface was well ordered. Details of the reduction mechanism and the particles leaving the surface in the course of the reduction process are not known. Recently, an X-ray induced reduction was reported for aluminovanadate oxides [34]. For the vanadyl-terminated surface, a partial removal of vanadyl groups during XPS measurements cannot be excluded. However, this effect was so small that it could not be detected with XPS which, admittedly, is not very sensitive to the removal of a small number of vanadyl groups. For the reduced surface, which was studied in more detail than the vanadyl-terminated surface, no

Dedicated to Prof. Konrad Hayek.

* To whom correspondence should be addressed.
E-mail: grupp@imc.tuwien.ac.at

signs of (further) reduction could be found. In any case, we emphasize that XPS was not employed in the course of the TDS investigations.

Compared to pristine V_2O_3 the "reduced" surface behaves differently with respect to molecular adsorption and reaction. Previous structure characterization [32] now allows for further studies of adsorption and reaction properties of V_2O_3. In this paper, we describe the interaction of CO, propane and propene with "oxidized" (vanadyl-terminated (V=O)), "reduced" (vanadium-terminated) and oxygen-pre-dosed reduced $V_2O_3(0001)$ surfaces. Although no significant surface reactions could be initiated under the applied conditions, combining TPD and XPS still provides information on the basic adsorption properties and the nature of surface sites.

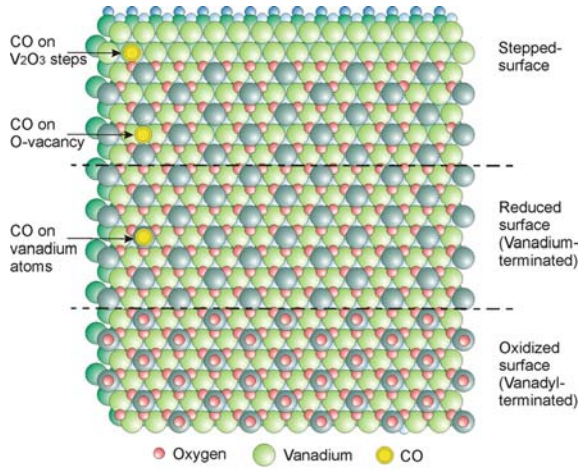

Scheme 1. Top view of oxidized (vanadyl-terminated), reduced (vanadium-terminated) $V_2O_3(0001)$ surfaces, oxygen vacancies and steps on the vanadium-terminated surface. Possible configurations of CO adsorbed on different sites are also shown.

2. Experimental

The experiments were performed in two separate UHV systems, one dedicated to TPD, the other to high resolution core level XPS. Both UHV systems (base pressure $\sim 1\times10^{-10}$ mbar) were equipped with an ion sputter gun for surface cleaning, metal evaporators and a quartz microbalance for thin film preparation, LEED and Auger electron spectroscopy (AES) for surface characterization, a source for electron bombardment, and a quadrupole mass spectrometer (QMS). The TPD system had a differentially pumped mass spectrometer (to avoid readsorption of molecules), the XPS system was located at the BESSY II electron storage ring (Berlin).

Sample preparation was, of course, performed identically in both systems. The Au(111) sample crystal was spot-welded by Ta wires to two Mo rods and could be heated resistively to 1000 K and cooled with liquid N_2 to 90 K. Clean Au(111) was obtained by cycles of Ar^+ bombardment (1 keV) at 300 K and annealing at 800 K for 5 min. The structure and cleanliness of the surface were confirmed by LEED and AES.

V_2O_3 films of about 10 nm thickness were prepared by evaporation of an equivalent of ~5 nm (metallic) vanadium (from a V rod) in 1×10^{-7} mbar oxygen at 600 K followed by annealing at 670 K (at the same pressure) for 15 min and final annealing at 850 K for 10 min. The well-ordered structure of the $V_2O_3(0001)$ film was confirmed by LEED at 90 K, showing a pattern as that reported in [19,32,33]. In the following we describe the different surfaces examined (scheme 1).

(i) *Oxidized surface*: The as-prepared surface is denoted "oxidized surface". This surface has been shown to exhibit vanadyl (V=O) group termination [19,32,33].

(ii) *Reduced surface*: The pristine $V_2O_3(0001)$ surface was reduced by electron irradiation at room temperature using a tungsten filament positioned in front of the sample (500 eV electrons for 30 s; current 5 mA). Electron bombardment removes the vanadyl oxygen atoms (or, at least, most of them) and produces a vanadium terminated surface [19,32,33].

(iii) *Oxygen pre-covered surface*: The reduced surface was exposed to 1–2 L (10^{-6} Torr s) oxygen at room temperature prior to the adsorption of the probe molecules.

For TPD measurements, the sample was placed at a distance of less than 1 mm in front of a differentially pumped quadrupole mass spectrometer. An aperture in front of the QMS eliminated desorption signals originating from the sample holder. The heating rate was 1 K/s for all experiments. CO was monitored via mass 28, propane (C_3H_8) via mass 29 (being the most intense fragment), and propene (C_3H_6) via mass 41. To illustrate the fragmentation of C_3H_8 and C_3H_6 in the QMS, mass spectra at 10^{-6} mbar pressure are shown in figure 1. The ion gauge readings were corrected according to the ion gauge sensitivities (CO: 1.1; C_3H_8, C_3H_6: 3.6).

XPS measurements were carried out at the BESSY II electron storage ring in Berlin with Scienta SES200 and Omicron EA125 analyzers utilized for data acquisition. C1s spectra were measured with 380 eV photons at an incidence angle of 55°.

3. Results

3.1. Adsorption of CO on $V_2O_3(0001)/Au(111)$

Adsorption of CO on pristine $V_2O_3(0001)$ films ("oxidized", with V=O termination) is rather limited. The small desorption peak at 105 K in the TPD spectrum shown in figure 2a is probably due to adsorption on a limited number of "defects", most likely sites where

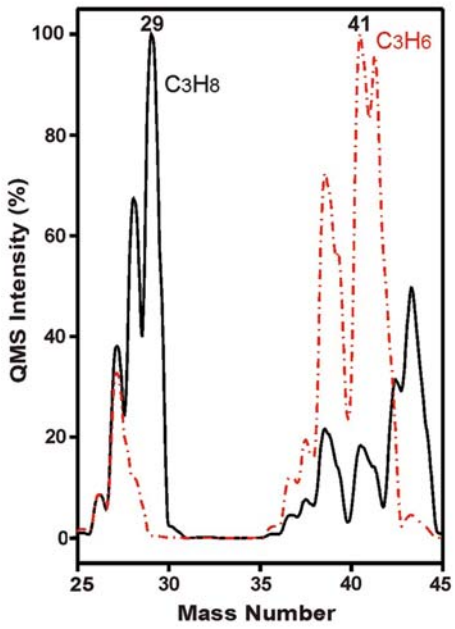

Figure 1. Mass (fragmentation) spectra of propane (solid line) and propene (dashed line) recorded at 10^{-6} mbar pressure.

the vanadyl oxygen is missing and V atoms are exposed. Corresponding temperature-dependent C1s XPS spectra are displayed in figure 2b. A small peak at 290.3 eV that mostly decreased between 90 and 140 K was observed, basically corroborating the TPD behavior.

In contrast, when the surface was reduced (removing most vanadyl oxygen atoms by electron irradiation) an intense desorption feature was observed at 120 K, with a shoulder at 190 K and a small high temperature desorption state at 330 K (figure 2a). Corresponding temperature-dependent C1s XPS signals from CO adsorbed on reduced V_2O_3 are shown in figure 2c, with a major signal at 289.9 eV and a smaller one at 287.3 eV. One may also note that the peak at 289.9 eV has a tail to higher binding energy. The spectrum could be fairly well fitted with three peaks at 287.3, 289.9 and 291.3 eV (not shown). The presence of three states is in good agreement with TPD. The peaks at 287.3 and 289.9 eV mostly disappeared around 150–200 K resembling the TPD peaks at 120 and 190 K. The feature at 291.3 eV exhibits weak intensity at 370 K which may parallel the desorption around 330 K.

The amount of CO adsorbed on the reduced surface is ~9–10 times higher than on the pristine (oxidized) V_2O_3 surface, as indicated both by the TPD peak areas and by integration of XPS signals (one should note that the XPS signals shown in figure 2b are multiplied by 4). Apparently, V=O groups hinder CO adsorption.

On the reduced surface the CO species desorbing at 120, 190 and 330 K follow a 70:25:5 ratio while XPS at 90 K indicated that the peaks at 289.9, 287.3 and 291.3 eV follow 60:30:10 ratio. The desorption feature at 120 K is attributed to CO adsorbed on vanadium atoms, which were accessible after the elimination of vanadyl oxygen atoms by electron irradiation (the strong TPD intensity of this band proves that the removal of vanadyl oxygen atoms is effective). The shoulder at 190 K is due to stronger bonded CO, that may be bonded at boundaries of neighboring V_2O_3 domains or at steps of a V_2O_3 terrace [35,36] (this assignment can currently not be proven though). The high temperature feature at 330 K is assigned to CO adsorption on strongly bonding defect sites such as O-vacancies in the first oxygen layer. A schematic of these sites is shown in scheme 1. When the reduced surface is exposed to oxygen, oxygen binds to the vanadium atoms and defect sites and the effect of reduction is mostly reversed (as observed by CO-TPD, not shown) [32].

The C1s binding energy (BE) of CO is quite high, i.e., shifted by several eV as compared to the BE of CO

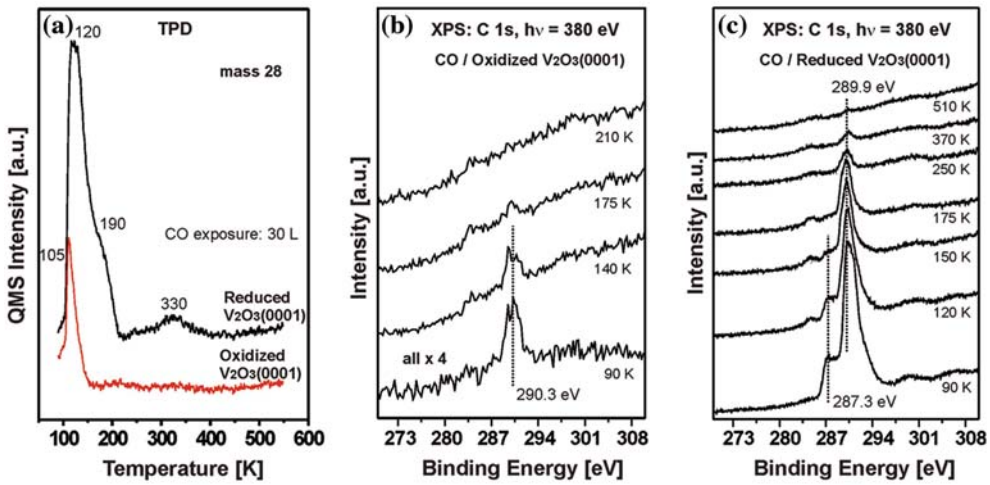

Figure 2. (a) TPD spectra of CO adsorbed on oxidized and reduced $V_2O_3(0001)$ surfaces. C1s XPS signals of CO on (b) oxidized and (c) reduced $V_2O_3(0001)$ surfaces, acquired after 30 L exposure at 90 K and subsequent annealing to the indicated temperatures.

adsorbed on metals [37–40]. The high CO binding energies both on oxidized and reduced V_2O_3 indicate that the bonding behavior is substantially different from that on metals. Similar shifts in binding energy have been reported for CO adsorbed on $Cr_2O_3(111)$ [41,42] and the present observation may involve similar effects. The interaction or coupling between CO adsorbed on V and underlying/neighboring oxygen atoms in V_2O_3 may induce the shift in binding energies. Alternatively, the shift may be due to the reduced screening of the final state on oxides, as compared to metals.

The intense C1s signal at 289.9 eV on the reduced surface (one may regard this as being shifted from 290.3 eV to lower BE) again indicates the removal of the vanadyl groups. However, the observed binding energies are higher than those reported for CO on V-oxide/Pd(111) by Netzer and co-workers [20,23,43 and references therein]. This may be due to the thickness (~10 nm) of the V_2O_3 film used in our study (i.e., there is no screening by the Au(111) substrate), while the V-oxide of Netzer *et al.* was around monolayer thickness. A high BE of 290 eV is also characteristic for gas phase CO [39] but this can be clearly excluded here, since the experiments were carried out under UHV. For V_2O_3, V can adopt different oxidation states (5+, 4+, 3+), due to the existence of different types of oxygen vacancies, which may further complicate the interpretation. An STM analysis of the exact V_2O_3 surface structure is in progress. Summarizing, CO may be a useful probe molecule that allows to titrate vanadyl groups (or rather their absence) on a V_2O_3 surface and, to some extent, to detect the presence of surface defects such as oxygen vacancies or step edges.

3.2. Adsorption of propane on $V_2O_3(0001)/Au(111)$

3.2.1. Oxidized surface

After adsorbing propane on the pristine $V_2O_3(0001)$ surface TPD indicated molecular propane desorption as major process. TPD data are displayed in figure 3a for different exposures at 90 K (propane was monitored via mass 29, which has the highest intensity in QMS). For an exposure of 0.1 L no desorption was observed. The desorption profile at 0.3 L exhibits a feature centered at 160 K, which grows upon 0.5 L exposure and also another feature appeared at 140 K. The 140 K feature grows with exposure and an intense (not saturable) peak appeared at 110 K. A fourth state was observed at 240 K for exposures greater than 1.0 L. No other desorbing species such as CO, CO_2, H_2, H_2O, or C_3H_6 were detected by TPD (taking into account and correcting for propane fragmentation).

As the low temperature peak at 110 K continues to grow with exposure without saturation, it can be attributed to propane multilayer desorption. The feature at 140 K with first order desorption kinetics is probably due to propane adsorption on vanadyl (V=O) sites,

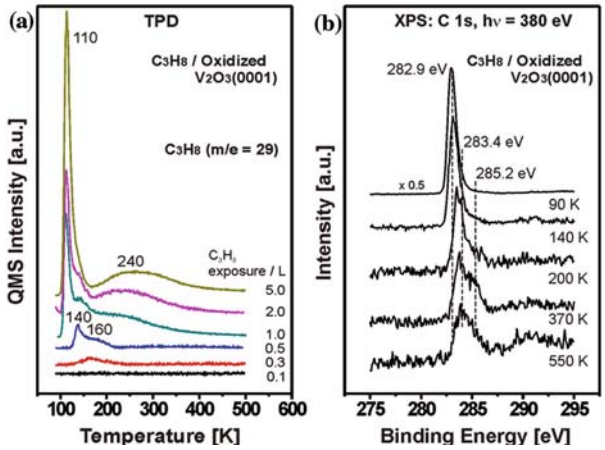

Figure 3. (a) TPD spectra of C_3H_8 adsorbed on oxidized $V_2O_3(0001)$. The surface was exposed to various amounts of propane at 90 K and heated at 1 K/s. (b) C1s XPS signals on oxidized $V_2O_3(0001)$, acquired after 30 L exposure at 90 K and subsequent annealing to the indicated temperatures.

since its considerable intensity rather rules out adsorption on defects. Propane may adsorb on these sites via C-vanadyl interaction and via H bonding between one H atom of a CH_3 group to oxygen of the V_2O_3 film, as proposed for propane adsorption on technical vanadia catalysts [1–3,10,11,44–48]. The feature at 160 K appearing at low exposure (0.3 L) is attributed to the adsorption of propane on defect sites (such as missing vanadyl oxygen atoms and/or oxygen vacancies in the first layer).

At first, the high desorption temperature of the feature at 240 K would suggest adsorption on defect sites. However, this state only appears at exposures ≥1.0 L and grows with coverage. This behavior was reproduced in repeated experiments and can thus not originate from changes in surface morphology during TPD. This is further supported by the reproducibility of the 0.3 L exposure TPD spectrum at the end of every TPD experiment and by LEED, which was unchanged even after several TPD cycles. Therefore, the high temperature feature at 240 K is tentatively assigned to recombinative desorption of propane. One possible mechanism is that at higher coverage part of the propane molecules dehydrogenate to propene, which recombines with hydrogen before desorption and then desorbs as propane.

Figure 3b shows C1s XPS spectra of oxidized $V_2O_3(0001)$ (vanadyl-terminated) after exposure to 30 L propane (C_3H_8) at 90 K, and subsequent heating to the indicated temperatures. The C1s spectrum at 90 K shows a very intense peak at 282.9 eV which has lost about half of its original intensity around 140 K, corresponding to propane multilayer desorption (paralleling the TPD peak at 110 K). The intensity of the XPS signal at 140 K suggests that there is still a considerable amount of propane present on the surface. The binding

energy of this species is lower than that reported for the molecular/multilayer adsorption of hydrocarbons on metal surfaces, which is around 284 eV [49–53]. The shift in binding energy to lower values indicates the different bonding behavior of propane on V_2O_3 as compared to that on metal surfaces. Thermal annealing to 200 K results in shifting the C1s peak to 283.4 eV and this value suggests propyl species. Similar alkyl species have been observed on Ni(100) (284.0 eV) [49,50], Pt(111) (283.7 eV) [51], Pd(110) (284.1 eV) [52], Cu(110) (284.5 eV) [53] and NiAl(110) (283.5 eV) [54]. Upon further annealing to temperatures higher than 300 K another peak at 285.2 eV was observed (see 370 K spectrum). The decrease in intensity that occurs around 300 K is attributed to desorption of propane (see figure 3a). However, according to TPD, there is (nearly) no propane desorption above 300 K. Hence, the remaining peaks at 283.4 and 285.2 eV at ≥370 K are most probably due to the presence of carbonaceous species (due to propane decomposition).

3.2.2. Reduced surface

TPD spectra of propane adsorbed on the reduced (V-terminated) $V_2O_3(0001)$ surface are shown in figure 4a for various amounts of propane adsorbed at 90 K. Again, desorption of the parent molecule (mass 29) was the predominant process. For the V-terminated surface differences were observed as compared to the (V=O)-terminated surface. A small desorption feature appeared at 135 K at 0.1 L exposure, continuously shifted to 120 K at 0.5 L and saturated around 1.0 L exposure. Upon higher exposure a feature at 110 K appeared and increased in intensity (without saturation). Very limited desorption occurred around 240 K at high exposure (inset in figure 4a), much less than that observed on the oxidized surface. No other desorption products were detected.

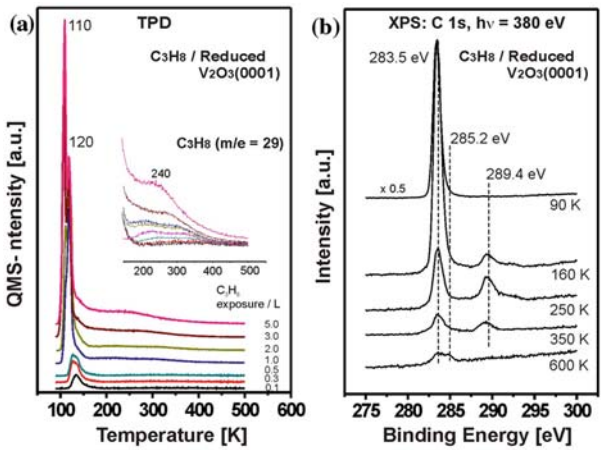

Figure 4. (a) TPD spectra of C_3H_8 adsorbed on reduced $V_2O_3(0001)$. The surface was exposed to various amounts of propane at 90 K and heated at 1 K/s. (b) C1s XPS signals on reduced $V_2O_3(0001)$, acquired after 30 L exposure at 90 K and subsequent annealing to the indicated temperatures.

The feature, which shifts from 135 K to 120 K with coverage is due to "regular" molecular propane adsorption on the V-terminated surface. It saturates around 1 L and at higher exposure a propane multilayer forms (desorption at 110 K). The 240 K feature is again quite small. The overall amount of propane adsorption is higher on the V-terminated surface than on the V=O terminated surface, i.e., vanadyl groups rather prevent propane adsorption. Propane may be oriented with the C–C–C chain parallel to the surface thus having weak interaction with the surface vanadium/oxygen atoms. Propane adsorption on the oxygen pre-adsorbed reduced surface showed similar results to those observed from the oxidized surface indicating that the V=O groups were re-established to some extent.

Figure 4b shows C1s XPS signals of reduced $V_2O_3(0001)$ after exposure to 30 L propane (C_3H_8) at 90 K, followed by subsequent heating to the indicated temperatures. The C1s spectrum at 90 K shows an intense peak at 283.5 eV. Compared to propane on the oxidized surface, the shift in binding energy to lower values is smaller, indicating a difference in bonding to oxidized and reduced surfaces (as the reduced surface does not have (many) vanadyl groups). As such, the interaction between propane and vanadyl oxygen should be the reason for the observed larger shift in binding energy on the oxidized surface (to 282.9 eV). The peak at 283.5 eV decreased in intensity upon annealing to 160 K, paralleling the TPD peaks at 110–135 K (desorption of molecularly adsorbed propane (multilayer/monolayer)). Because desorption of molecular propane is mostly complete around 150 K, the presence and the binding energy of the 283.5 eV peak at 160 K suggests alkyl-like species on the surface, as discussed above. Thermal annealing ≥160 K further decreased the 283.5 eV intensity and also resulted in the appearance of a second peak at 289.4 eV, which disappeared at temperatures higher than 400 K. The 289.4 eV peak is tentatively assigned to adsorbed CO (from the residual gas) but may also partly be due to a C–O containing species (via reaction of propane with a surface oxygen). In any case, it is only a few % of the initial propane signal.

Annealing to temperatures higher than 400 K produced another small peak at 285.2 eV (see 600 K spectrum). This feature and the remaining intensity around 283.5 eV are most probably due to carbonaceous residues.

3.3. Adsorption of propene on $V_2O_3(0001)/Au(111)$

3.3.1. Oxidized surface

On vanadyl-terminated $V_2O_3(0001)$ mainly molecular desorption of propene was observed. Figure 5a displays propene TPD spectra (monitoring mass 41) for different exposures at 90 K. At the initial exposure of 0.3 L a peak was observed at 120 K, which increased and

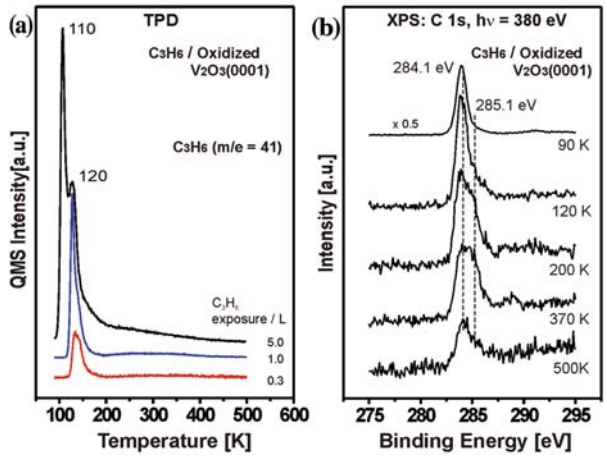

Figure 5. (a) TPD spectra of C_3H_6 adsorbed on oxidized $V_2O_3(0001)$. The surface was exposed to various amounts of propene at 90 K and heated at 1 K/s. (b) C1s XPS signals on oxidized $V_2O_3(0001)$, acquired after 30 L exposure at 90 K and subsequent annealing to the indicated temperatures.

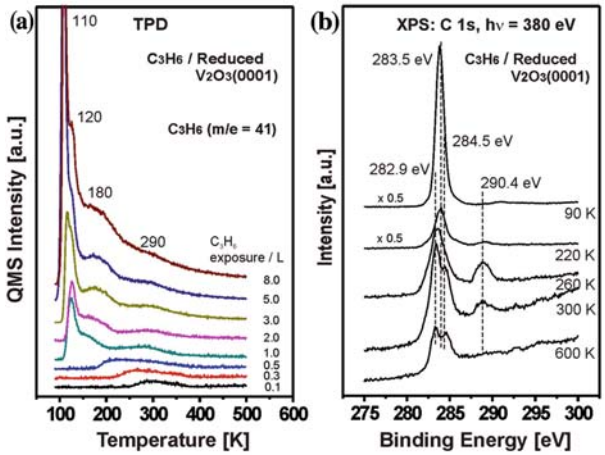

Figure 6. (a) TPD spectra of C_3H_6 adsorbed on reduced $V_2O_3(0001)$. The surface was exposed to various amounts of propene at 90 K and heated at 1 K/s. (b) C1s XPS signals on reduced $V_2O_3(0001)$, acquired after 30 L exposure at 90 K and subsequent annealing to the indicated temperatures.

saturated at 1 L. At higher exposure a second peak developed at 110 K and increased continuously with exposure, suggesting propene multilayer desorption. The signal at 120 K is attributed to "regular" propene adsorption on the V=O terminated surface. No other desorbing species were detected. Compared to *propane* adsorption on the oxidized surface, the interaction with propene is more favorable (considering that the 120 K peak for propene is ~4 times larger than the 140 K peak for propane). For Pd(111) Thornbug *et al.* reported desorption of molecular propene only (upon propene adsorption at low temperature) showing that dissociation or other surface reactions seem not to occur on metal (at least Pd) sites [55].

Figure 5b displays C1s XPS signals of oxidized V_2O_3 after exposure to 30 L propene at 90 K and subsequent heating to the indicated temperatures. At 90 K, an intense peak corresponding to multilayer/monolayer propene was observed at 284.1 eV. Thermal annealing to 120 K results in an intensity decrease with the appearance of a shoulder at 285.1 eV. Both peaks can then be observed up to about 500 K, with a reduction of intensities, and disappeared above 550 K. According to TPD, propene multilayers desorb at 110 K (see figure 5a) explaining the intensity loss of the C1s signal at 284.1 eV at 120 K. A monolayer of propene is stable on the surface up to ~150 K (see TPD spectra) and hence the remaining C1s signals at 284.1 and 285.1 eV at higher temperature suggest the presence of alkyl/carbonaceous species on the surface. On Pt(111) multilayer and molecular propene were observed at 284.6 and 283.6 eV, respectively [56].

3.3.2. Reduced surface

TPD spectra of propene desorption from the reduced (V-terminated) surface after exposure to various amounts of propene at 90 K are shown in figure 6a. Again, desorption of the parent molecule (mass 41) was the predominant process. For the reduced surface major differences occurred as compared to the oxidized surface. A small desorption feature appeared at 290 K at 0.1 L exposure. A second peak at 180 K is established around 1.0 L, together with a strong signal at 120 K which saturated at ~3 L. Above 3 L, a continuously growing feature at 110 K appeared. No other species such as CO, CO_2, H_2, H_2O, or C_3H_8 were detected by TPD.

The low temperature (non-saturating) desorption feature at 110 K indicates propene multilayer adsorption. The peak at 120 K is due to "regular" propene adsorption on the V-terminated surface [1–3,10,11,44–48,57,58]. The high temperature desorption signals at 180 K and 290 K most likely originate from propene desorption from defects such as oxygen vacancies or domain boundaries and step edges.

Figure 6b displays C1s XPS signals of reduced V_2O_3 after exposure to 30 L propene at 90 K and subsequent heating to the indicated temperatures. At 90 K, an intense peak corresponding to multilayer/monolayer propene was observed at 283.5 eV. Thermal annealing to 120 K resulted in an intensity decrease and further annealing to 220 K produced another small peak at 290.4 eV. When the temperature was above 250 K, the signal at 283.5 eV shifted to 282.9 eV. At 300 K another peak appeared at 284.5 eV. Further annealing up to 600 K resulted in the disappearance of the 290.4 eV peak while the signals at 282.9 and 284.5 eV remained.

The large intensity reduction around 120 K suggests desorption of the propene multilayer. The remaining intensity (e.g., at 220 K) is attributed to adsorbed (monolayer) propene (correlated with the species desorbing at ~180 K). The C1s signals at 282.9 and

284.5 eV suggest the presence of alkyl and/or carbonaceous species, produced by propene decomposition at higher temperature. Alternatively, the latter two species may still originate from propene bonded to different defect sites (the characterization of which is subject of future STM experiments). The 290.4 eV signal is again attributed to adventitious CO (or to an unidentified C–O containing species). It should be noted here that on the reduced surface propene overall has a somewhat higher thermal stability (cf. figures 5a and 6a).

Compared to *propane*, the propene coverage is about twice as much and the TPD desorption temperatures are also higher (taking into account defect-related desorption). This indicates a stronger interaction of *propene* with the reduced surface, indicating that π-bonding favors adsorption. XPS showed a similar trend in that the intensities of the propene signals were higher than those observed for propane. On the oxygen pre-covered reduced surface TPD features similar to those for the oxidized surface were observed.

3.4. Reaction at mbar pressure

The results presented above show that CO, propane and propene bind stronger to the reduced V-terminated $V_2O_3(0001)$ surface than to the oxidized surface (which exhibits V=O termination). Nevertheless, vanadyl groups are probably required in the course of catalytic reactions. In the past, studies of propane oxidative dehydrogenation (ODH) to propene on technical V_2O_5 catalyst suggested that the reaction proceeds via reduction of V^{5+} sites to V^{4+} (and V^{3+}) [1–3,7]. Nevertheless, some reactivity may also be observed for V_2O_3 under real catalytic reactions, i.e., in the presence of high oxygen pressure. Therefore, we have also carried out catalytic reactions at atmospheric pressure on both oxidized and reduced V_2O_3 model surfaces (50 mbar C_3H_8, 50 mbar O_2, He up to 1 bar), at temperatures up to 500 K. However, the oxidation state of the surfaces, in particular the stability of the reduced surface in a high oxygen pressure, have not been examined yet and are subject of further studies. In any case, no reaction products were observed by gas chromatography, which might in part be due to the low reaction rates on vanadium oxide surfaces. Temperature programmed reaction spectroscopy is an alternative route to examine model catalyst activity and such experiments are currently performed.

4. Conclusions

The adsorption of CO, propane and propene was monitored by temperature programmed desorption (TPD) and X-ray Photoelectron Spectroscopy (XPS) on "oxidized" (vanadyl-terminated (V=O)), "reduced" (vanadium-terminated) and oxygen-covered reduced $V_2O_3(0001)$ surfaces. For all molecules TPD indicated stronger bonding to the vanadium-terminated surface and contributions of high temperature desorption states originating from various kinds of surface defects, presumably oxygen vacancies or domain boundaries/step edges. XPS observations fairly agree with the TPD results but also revealed a high complexity, e.g., contributions of dehydrogenation reactions, that is currently not fully understood.

Acknowledgment

A.B. is grateful for an Alexander von Humboldt fellowship.

References

[1] K. Chen, E. Iglesia and A.T. Bell, J. Catal. 192 (2000) 197.
[2] K. Chen, A.T. Bell and E. Iglesia, J. Phys. Chem. B 104 (2000) 1292.
[3] T. Blasco and J.M. Lopez Nieto, Appl. Catal. A 157 (1997) 117.
[4] M.E. Harlin, V.M. Niemi and A.O.I. Krause, J. Catal. 195 (2000) 67.
[5] G.S. Wong, D.D. Kragten and J.M. Vohs, Surf. Sci. 452 (2000) L293.
[6] Q. Wang and R.J. Madix, Surf. Sci. 496 (2002) 51.
[7] T. Feng and J.M. Vohs, J. Phys. Chem. B 109 (2005) 2120.
[8] D.R. Justes, N.A. Moore and A.W. Castleman Jr., J. Phys. Chem. B 108 (2004) 3855.
[9] B.P. Barbero, L.E. Cadus and L. Hilaire, Appl. Catal. A 246 (2003) 237.
[10] T. Ono, Y. Tanaka, T. Takeuchi and K. Yamamoto, J. Mol. Catal. A 159 (2000) 293.
[11] K. Routray, K.R.S.K. Reddy and G. Deo, Appl. Catal. A 2655 (2004) 103.
[12] T. Feng and J.M. Vohs, J. Catal. 221 (2004) 619.
[13] S. Surnev, M.G. Ramsey and F.P. Netzer, Progr. Surf. Sci. 73 (2003) 117.
[14] C. Klein, G. Kresse, S. Surnev, F.P. Netzer, M. Schmid and P. Varga, Phy. Rev. B 68 (2003) 235416.
[15] J. Schoiswohl, S. Surnev, M. Sock, S. Eck, M.G. Ramsey and F.P. Netzer, Phy. Rev. B 71 (2005) 165437.
[16] B. Sass, T. Tusche, W. Felsch, N. Quaas, A. Weismann and M. Wenderoth, J. Phys.: Condens Matter 16 (2004) 77.
[17] S. Surnev, G. Kresse, M. Sock, M.G. Ramsey and F.P. Netzer, Surf. Sci. 495 (2001) 91.
[18] J. Schoiswohl, M. Sock, S. Surnev, M.G. Ramsey, F.P. Netzer, G. Kresse and J.N. Andersen, Surf. Sci. 555 (2004) 101.
[19] A.-C. Dupuis, M. Abu Haija, B.H. Richter, H. Kuhlenbeck and H.-J. Freund, Surf. Sci. 539 (2003) 99.
[20] S. Surnev, M. Sock, G. Kresse, J.N. Andersen, M.G. Ramsey and F.P. Netzer, J. Phys. Chem. B 107 (2003) 4777.
[21] M. Casarin, M. Nardi and A. Vittadini (2004) Surf. Sci. 566–568:451.
[22] T. Tepper, B. Richter, A.-C. Dupuis, H. Kuhlenbeck, C. Hucho, P. Schilbe, M.A. bin Yarmo and H.-J. Freund, Surf. Sci. 496 (2002) 64.
[23] M. Sock, S. Surnev, M.G. Ramsey and F.P. Netzer, Topics Catal. 14 (2001) 15.
[24] G. Kresse, S. Surnev, J. Schoiswohl and F.P. Netzer, Surf. Sci. 55 (2004) 118.
[25] A. Kämper, I. Hahndorf and M. Baerns, Topics Catal. 11/12 (2000) 77.

[26] A. Kämper, A. Auroux and M. Baerns, Phys. Chem. Chem. Phys. 2 (2000) 1069.
[27] I. Czekaj, M. Witko and K. Hermann, Surf. Sci. 525 (2003) 33; Surf. Sci. 525 (2003) 45; Surf. Sci. 555 (2003) 85.
[28] C. Kolczewski and K. Hermann, Theor. Chem. Acc. 114 (2005) 60.
[29] N. Magg, B. Immaraporn, J.B. Giorgi, T. Schroeder, M. Bäumer, J. Dobler, Z. Wu, E. Kondratenko, M. Cherian, M. Baerns, P.C. Stair, J. Sauer and H.-J. Freund, J. Catal. 226 (2004) 88.
[30] (a) K. Hayek, M. Fuchs, B. Klötzer, W. Reichl and G. Rupprechter, Topics Catal. 13 (2000) 55. (b) K. Hayek, B. Jenenwein, B. Klötzer and W. Reichl, Topics Catal. 14 (2001) 25. (c) W. Reichl and K. Hayek, J. Catal. 208 (2002) 422.
[31] (a) S. Penner, D. Wang, R. Schlögl and K. Hayek, Thin Solid Films. 484 (2005) 10. (b) S. Penner, B. Jenewein, D. Wang, R. Schlögl and K. Hayek, Phys. Chem. Chem. Phys. 8 (2006) 1223.
[32] M. Abu Haija, S. Guimond, A. Uhl, H. Kuhlenbeck and H.-J. Freund, Surf. Sci. 600 (2006) 1040.
[33] (a) S. Guimond, M. Abu Haija, S. Kaya, J. Lu, J. Weissenrieder, Sh. K. Shaikhutdinov, H. Kuhlenbeck, H.-J. Freund, J. Döbler and J. Sauer, Topics Catal. 38 (2006) 117. (b) M. Abu Haija, S. Guimond, A. Uhl, H. Kuhlenbeck, H.-J. Freund, T.K. Todorova, M.V. Ganduglia-Pirovano and J. Döbler, J. Sauer Surf. Sci. 600 (2006) 1497.
[34] S.P. Chenakin, R. Prada Silvy and N. Kruse, Catal. Lett. 102 (2005) 39.
[35] N. Magg, J.B. Giorgi, M.M. Frank, B. Immaraporn, T. Schroeder, M. Bäumer and H.-J. Freund, J. Am. Chem. Soc. 126 (2004) 3616.
[36] M. Beutl and J. Lesnik, Vacuum 61 (2001) 113.
[37] H. Conrad, G. Ertl, J. Koch and E.E. Latta, Surf. Sci. 43 (1974) 462.
[38] F.P. Leisenberger, S. Surnev, L. Vitali, M.G. Ramsey and F.P. Netzer, J. Vac. Sci. Technol. A17 (1999) 1743.
[39] V.V. Kaichev, I.P. Prosvirin, V.I. Bukhtiyarov, H. Unterhalt, G. Rupprechter and H.-J. Freund, J. Phys. Chem. B 107 (2003) 3522.
[40] D. Schmeisser, F. Greuter, E.W. Plummer and H.-J. Freund, Phys. Rev. Lett. 54 (1985) 2095.
[41] C. Xu, B. Dillmann, H. Kuhlenbeck and H.-J. Freund, Phys. Rev. Lett. 67 (1991) 3551.
[42] M. Pykary, V. Staemmler, O. Seiferth and H.-J. Freund, Surf. Sci. 479 (2001) 11.
[43] J. Schoiswahl, S. Eck, M.G. Ramsey, J.N. Andersen, S. Surnev and F.P. Netzer, Surf. Sci. 580 (2005) 122.
[44] R. Graboski, S. Pietrzyk, S. Sloczynski, F. Genser, K. Wcislo and B. Grzybowska-Swierkosz, Appl. Catal. A 232 (2002) 277.
[45] G. Martra, F. Arena, S. Coluccia, F. Frusteri and A. Parmaliana, Catal. Today 63 (2000) 197.
[46] C. Resini, T. Montanari, G. Busca, J.-M. Jehng and I.E. Wachs, Catal. Today 99 (2005) 105.
[47] T.C. Watling, G. Deo, K. Seshan, I.E. Wachs and J.A. Lercher, Catal. Today 28 (1996) 139.
[48] A.A. Lemonidou, L. Nalbandian and I.A. Vasalos, Catal. Today 61 (2000) 333.
[49] S. Tjandra and F. Zaera, Surf. Sci. 289 (1993) 255.
[50] S. Tjandra and F. Zaera, J. Phys. Chem. B 101 (1997) 1006.
[51] F. Zaera, Surf. Sci. 219 (1989) 453.
[52] M. Bowker, M. Morgan, N. Perkins, R. Holroyd, E. Fourre, F. Grillo and A. MacDowall, J. Phys. Chem. B 109 (2005) 2377.
[53] K. Weiss, H. Öström, L. Triguera, H. Ogasawara, M.G. Garnier, C.G.M. Pettersson and A. Nilsson, J. Electr. Spectrosc. Rel. Phenom. 28 (2003) 179.
[54] S. Chaturred and D.R. Strongin, J. Vac. Sci. Technol. A 17 (1999) 810.
[55] N.A. Thornbug, I.M. Abdelrehim and D.P. Lard, J. Phy. Chem. B 103 (1999) 8894.
[56] A.F. Lee, K. Wilson, A. Goldoni, R. Larciprete and S. Lizzt, Surf. Sci. 513 (2002) 140.
[57] H. Yoshida, C. Murata and T. Hattori, J. Catal. 194 (2000) 364.
[58] W.X. Huang and J.M. White, Langmuir 18 (2002) 9622.